Radiance and Polarization of Light Reflected from Optically Thick Clouds

G. W. Kattawar and G. N. Plass

The reflected radiance and polarization are calculated for clouds with optical thicknesses from 10 to 100. The results are presented for both the haze C and nimbostratus model. The peak in the single scattered polarization at 140° for the nimbostratus model persists even with all the multiple scattering events that occur for the largest optical thicknesses considered here. The calculations are made by a Monte Carlo technique, which includes the effect of multiple scattering through all orders and a realistic anisotropic phase function for single scattering appropriate for the distribution of particle sizes in the cloud. The effect of the surface albedo is included in the calculations for the optical thickness of 10. The variation of the radiance and polarization with both the nadir and azimuthal angle is given for several solar zenith angles.

Introduction

Photons reflected from an optically thick cloud have, on the average, undergone a large number of scattering events. Many theoretical methods which are applicable for small optical depths cannot be used in practice when the optical depth becomes appreciably larger than unity. Furthermore, some of these methods apply only to isotropic or Rayleigh scattering functions and cannot be used with the highly anisotropic scattering functions that occur with water droplets at visible wavelengths.

Among the theoretical methods which are applicable to large optical depths is the doubling principle described by van de Hulst and Grossman[1] and used by Hansen[2−4] in several papers. A set of simple formulas and a table checked by a Monte Carlo calculation have been given by Danielson *et al.*[5] A Neumann series solution together with the doubling method have been used by Uesugi and Irvine[6] and by Irvine.[7] A matrix method based on a discrete set of zenith angles has been developed by Twomey *et al.*[8] Although it is possible that some of these methods can be extended to include polarization effects, these authors[1−8] discuss only the calculation of the radiance.

The radiance of the reflected and transmitted photons in the visible from thick cloud layers has been measured by Neiburger,[9] Ruff *et al.*,[10] Salomonson,[11] and Brennan and Bandeen.[12] It is difficult to compare their results with theoretical calculations, since the relevant parameters (such as size distribution and type of particles, number density of particles, and distribution with height) are not usually measured at the same time as the radiance.

Both the radiance and polarization of the photons that undergo multiple scattering in a cloud can be calculated by a Monte Carlo method. We have developed this method in a series of papers[13−17] and have reported values for the radiance and polarization for optical thicknesses up to 10. Unless sophisticated variance reduction techniques are used, the Monte Carlo method is inefficient at all optical thicknesses and impractical for large optical thicknesses. Such techniques have been used in our code so that it is now possible to obtain both the radiance and polarization of the reflected photons for optical thicknesses as large as 100, with reasonable computation times.

Method

The Monte Carlo method follows the accurate three-dimensional path of the photon as it undergoes multiple scattering by the water droplets in the cloud as well as reflection from the ground back into the cloud. The scattering angles are selected from the exact angular scattering matrix as calculated from Mie theory. The strong forward peak in the scattering function is accurately taken into account. The results include all orders of scattering and any number of reflections from the ground surface that make any contribution to the radiance. The ground is assumed to be represented by a Lambert surface. The effects due to the cloud alone are studied in this paper; thus scattering and absorption by atmospheric molecules are not included here.

The water droplets are represented by spherical particles with a real index of refraction of 1.33. Two

The authors are with the Physics Department, Texas A&M University, College Station, Texas 77843.

Received 21 May 1970.

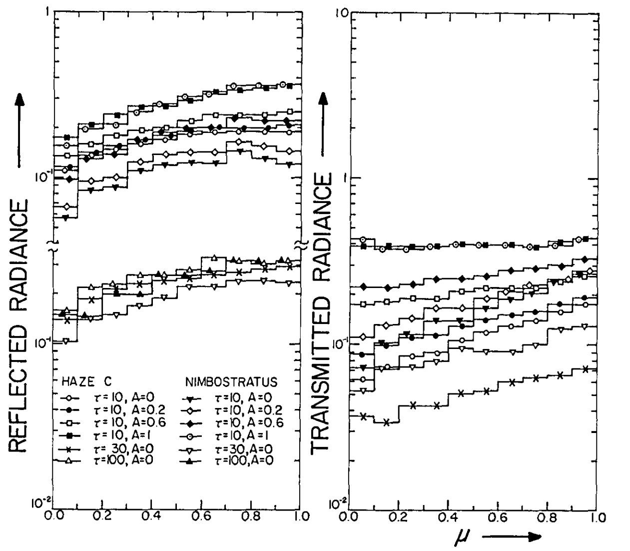

Fig. 1. Reflected and transmitted radiance as a function of cosine (μ) of nadir or zenith angle for haze C and nimbostratus models for cloud optical thickness (τ) of 10, 30, 100 and for surface albedo (A) of 0, 0.2, 0.6, and 1. The cosine (μ_0) of the solar zenith angle is -1 (sun at zenith). The incoming solar flux is normalized to unity.

size distributions are used here. One is the nimbostratus model[15] with a particle concentration proportional to $r^6 \exp(-0.5r)$. The maximum of this distribution occurs when the particle radius is 12 μ. The second distribution is the haze C model proposed by Deirmendjian[18] which has a constant particle concentration when $0.03\ \mu < r < 0.1\ \mu$ and a particle concentration proportional to r^{-4} when $r > 0.1\ \mu$. This corresponds to a continental haze with the typical r^{-4} variation in the number of particles. The average value of the cosine of the scattering angle is 0.868 for the nimbostratus model and 0.743 for the haze C model.

The scattering matrix for both of these size distributions was calculated exactly from the Mie theory[19] for a wavelength of 0.7 μ. The elements of the scattering matrix are shown for both of these models in Figs. 5 and 6 of Ref. 20. The Rubenson definition of the degree of polarization as the difference between the intensity in each of the two directions of polarization divided by their sum is used here. When it is positive, the plane of polarization of the scattered light is perpendicular to the scattering plane. We also calculated the polarization from the definition which involves the four components of the Stokes vector; the difference in the results obtained from these two definitions is very small for the cases given here.

The Monte Carlo code which includes polarization has been described by Kattawar and Plass.[20] Briefly, the four-component Stokes vector is obtained after each scattering event from the vector before scattering from an appropriate matrix transformation. This matrix involves the four independent components of the scattering matrix previously calculated from Mie theory. Both the polar angles that describe the angle of scattering are chosen from approximate distributions. However, the weight associated with each photon is multiplied by an appropriate factor, so that the final result is exactly the same as though the angles had been chosen from the correct bivariate distribution.

Collisions are forced so that the photon never leaves the atmosphere; the weight associated with the photon is changed each time a forced collision occurs so that the correct result is obtained. The photons are followed until their weight is so small that they make a negligible contribution to any of the detectors. Reflection from the planetary surface is taken into account by a special method which is equivalent to following a photon through an infinite number of collisions and reflections from the assumed Lambert surface. All the methods used in the Monte Carlo program have been thoroughly checked against calculations made from the exact radiative transfer equations. It should be emphasized that the exact three-dimensional path of the photon is followed in the Monte Carlo method and that the only averaging is done at the detectors, where the radiance is necessarily averaged over finite intervals of solid angle. For large optical depths, the method of Russian roulette is also used. Imaginary planes are introduced in the medium, and a probability equal to the fraction of the photons allowed to cross the plane is assigned. A photon approaching such a plane has its trajectory terminated if a random number is larger than the assigned probability; however, the trajectory continues if it is less. The weight of the photon is adjusted in the latter case by the factor of the reciprocal of the assigned probability.

Results

The radiance and polarization were calculated for optical thickness $\tau = 10$, 30, and 100 for both the nimbostratus and haze C models. A typical run, which takes 20 min on the CDC 6600 computer, calculates 27,000 photon histories and 900,000 collisions when $\tau = 10$. This calculation includes the photons that are reflected from the planetary surface so that results are obtained for six values of the planetary albedo. When

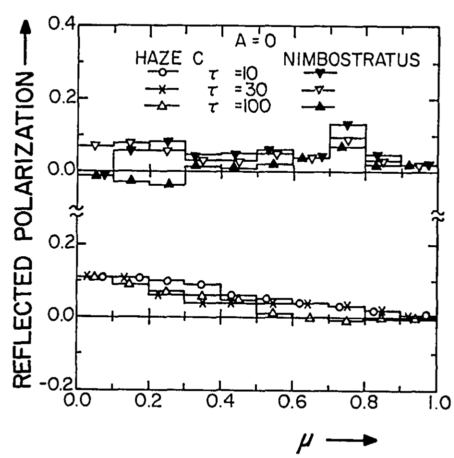

Fig. 2. Polarization of reflected radiation as a function of μ for haze C and nimbostratus models for $\tau = 10, 30, 100$; $A = 0$; $\mu_0 = -1$.

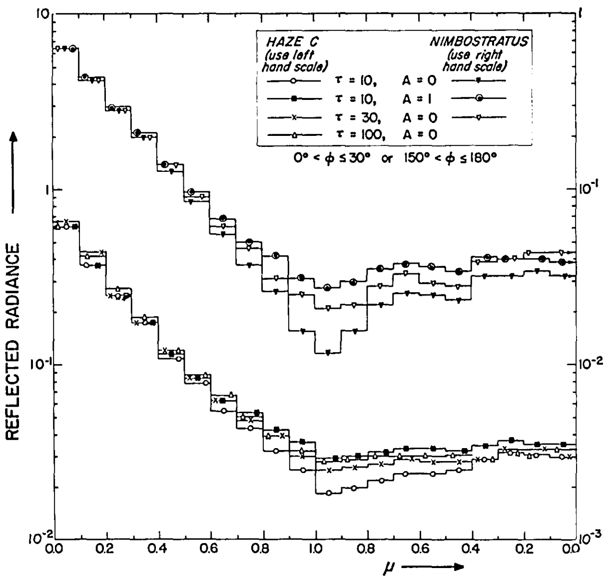

Fig. 3. Reflected radiance as a function of μ for $\mu_0 = -0.15$, $\tau = 10$, 30, and 100, $A = 0$ and 1. The results have been averaged over the azimuthal angles in the range $0° < \phi \leq 30°$ or $150° < \phi \leq 180°$. On all curves the solar horizon is on the left-hand side of the figure and the antisolar horizon is on the right-hand side.

$\tau = 100$, 5200 photon histories and 800,000 collisions are calculated in 15 min; here the planetary surface is assumed to have zero albedo, since its effect on the reflected photons is small for this large optical depth.

The reflected and transmitted radiance shown in Fig. 1 are for the case where the cosine of the solar zenith angle $\mu_0 = -1$ (sun at zenith). The curves for the reflected radiance when $\tau = 10$ are shown in the upper part of the left-hand figure; those for the larger values of τ are plotted in the lower part of the figure. Note the break in the scale for the ordinate. When $\tau = 10$, the surface albedo A still has an appreciable influence on the reflected radiance; it may be larger by as much as a factor of 2 when $A = 1$ than when $A = 0$ for the haze C model. The dependence on surface albedo is even larger for the nimbostratus model. The greater number of small angle scattering events in the nimbostratus model, compared to the haze C model, allows more photons to penetrate deeper into the medium; thus the dependence on the surface albedo is greater. When curves for the same surface albedo, but different models, are compared, it is found that the reflected radiance is always less for the nimbostratus model than for the haze C model and that the difference becomes larger as the surface albedo decreases.

In order to save computing time, the calculations for $\tau = 30$ and 100 were only made with a surface albedo of zero. When $\tau = 30$, the reflected radiance is always greater for the nimbostratus model than for the haze C model. The differences are not nearly so pronounced when $\tau = 100$. Previous studies have shown[14,15] that the reflected radiance may typically be 40% and 15% larger when $A = 1$ than when $A = 0$ for $\tau = 30$ and 100, respectively.

The transmitted radiance when $\tau = 100$ depends strongly on the surface albedo. When $A = 0$, there is a minimum for the transmitted radiance at the horizon. As A increases, the curve becomes flatter. Except when $A = 1$, the transmitted radiance is appreciably larger for the nimbostratus than for the haze C models. The difference is even larger when $\tau = 30$. The Monte Carlo results for the transmitted radiance for $\tau = 100$ are not shown, because so few photons penetrate such a thick cloud that the statistical fluctuation of the results is large.

The polarization of the reflected photons is shown in Fig. 2. The upper set of curves is for the nimbostratus model, whereas the lower set is for the haze C model. The polarization for the haze C model decreases fairly uniformly from a value of about 0.11 at the horizon to a very small value near the nadir. The polarization for this model calculated from single scattering alone is shown in Fig. 15 of Ref. 20. It has a value of nearly 0.5 near the horizon and decreases uniformly toward the nadir until a small negative region is reached at nadir angles smaller than 12°. For thick clouds, the multiple scattering reduces the polarization by approximately a factor of 0.4 near the horizon and by similar amounts elsewhere.

The polarization calculated for single scattering for the nimbostratus model is also shown in Fig. 15 of Ref. 20. It is quite irregular compared to the haze C curve and has a pronounced peak of about 0.8 in the range $0.7 < \mu < 0.8$; this corresponds to the rainbow angle. The value of the single scattered polarization is in the range from 0.4 to 0.5 for viewing angles near the horizon. This is reduced by a factor of 5 or 6 by multiple scattering (the few negative values from the Monte Carlo calculations near the horizon are probably statistical fluctuations, since these are always largest at these

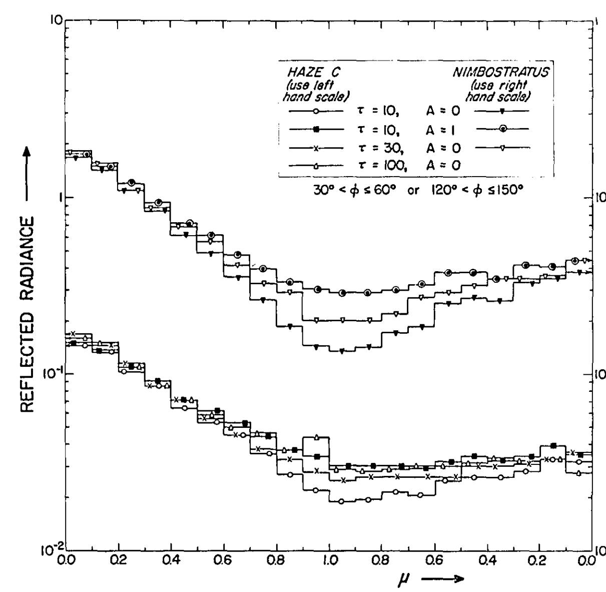

Fig. 4. Reflected radiance as a function of μ. Same as Fig. 3 except that the range of the azimuthal angle is $30° < \phi \leq 60°$ or $120° < \theta \leq 150°$.

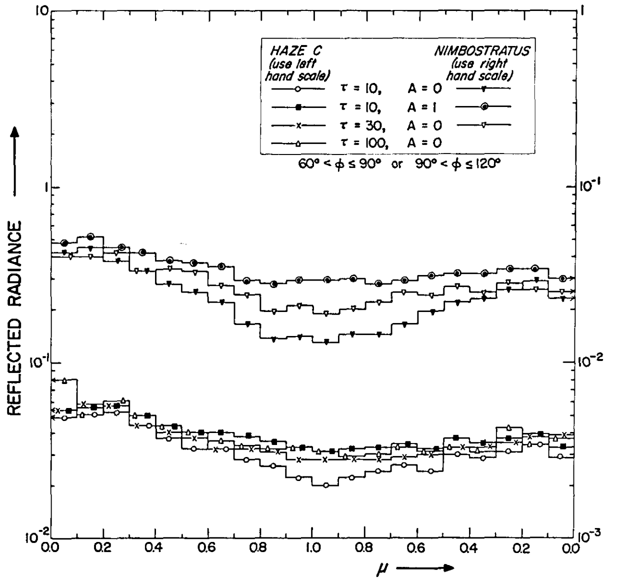

Fig. 5. Reflected radiance as a function of μ. Same as Fig. 3 except that the range of the azimuthal angle is $60° < \phi \leq 120°$.

angles). It is interesting that the peak in the range $0.7 < \mu < 0.8$ shows clearly for clouds of all optical thicknesses. Similarly the minimum near $\mu = 0.4$ is real and occurs in the single scattered polarization.

The reflected radiance is shown in Figs. 3–5 for $\mu = -0.15$. The solar horizon is on the left-hand side of these figures, the nadir is at the center, and the antisolar horizon is on the right-hand side. The curves of Fig. 3 have been averaged over the azimuthal angle ϕ in the range $0° < \phi \leq 30°$ or $150° < \phi \leq 180°$. The curves in Figs. 4 and 5 are for other azimuthal angles as marked. Thus the curves in Fig. 3 are for the reflected photons that leave the cloud in a plane through the nadir direction that makes an angle of less than 30° with the incident plane. The curves for the nimbostratus and haze C models have been plotted with a different origin in order to separate them. The right-hand scale should be used for the nimbostratus model and the left-hand scale for the haze C model. For the range of azimuthal angles used in Fig. 3, the reflected radiance depends most strongly on the optical depth of the cloud for angles near the nadir. It increases by almost a factor of 3 when τ increases from 10 to 30 for the nimbostratus model and for angles near the nadir.

Similar curves for the reflected radiance are shown in Fig. 4 for $30° < \phi \leq 60°$ or $120° < \phi \leq 150°$ and in Fig. 5 for $60° < \phi \leq 120°$. In all cases the most rapid variation of the reflected radiance as a function of τ occurs for the nimbostratus model for directions near the nadir. When the azimuthal angle is near 90°, the curves become relatively flat and depend little on the nadir angle.

The polarization of the reflected photons is given in Figs. 6–8 for $\mu_0 = -0.15$. The nimbostratus curves have been shifted upward with respect to the haze C curves for clearer viewing. The left-hand scale should be used for the haze C curves and the right-hand scale for the nimbostratus curves. The surface albedo is assumed to be zero for all of these curves. For these large optical thicknesses, the polarization is rather insensitive to the value of the surface albedo. For example, for the haze C model and $\tau = 10$, the polarization is -0.0052, $+0.076$, and -0.088 for the μ interval nearest the solar horizon, nadir, and antisolar horizon, respectively, when $A = 0$; the corresponding values when $A = 1$ are -0.0051, $+0.054$, and -0.076, respectively.

It is interesting to compare the polarization of the reflected photons for the haze C model for large τ values as shown in Figs. 6–8 with the same quantity for smaller τ values, i.e., $\tau = 0.1$ and 1, given in Figs. 16 and 17 of Ref. 20. The maximum value for the polarization decreases from about 0.3 when $\tau = 0.1$ and $\mu_0 = -0.1$ to values around 0.05 for large values of τ and $\mu_0 = -0.15$. However, the general character of the curve for $0° \leq \phi \leq 30°$ or $150° < \phi \leq 180°$ remains the same as τ increases; the polarization is negative near both the solar and antisolar horizons and positive in between with a maximum near the nadir. The only

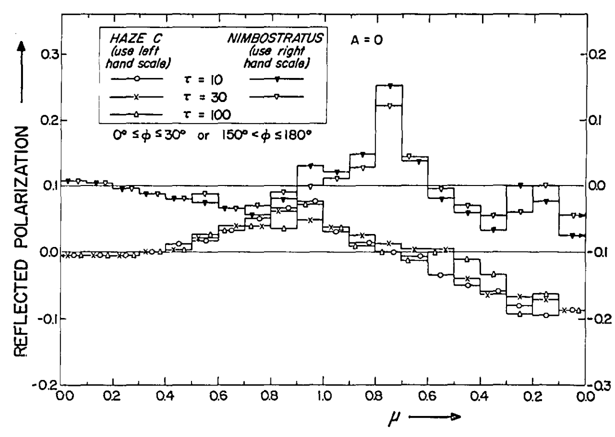

Fig. 6. Polarization of reflected radiation as a function of μ for $\mu_0 = -0.15$, $\tau = 10, 30$, and 100, $A = 0$, and $0° \leq \phi < 30°$ or $150° < \phi \leq 180°$.

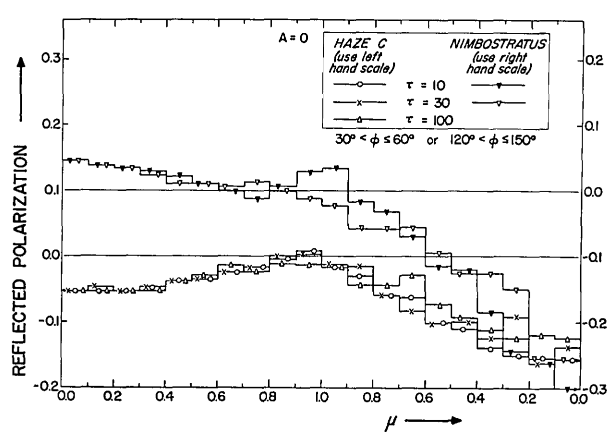

Fig. 7. Polarization of reflected radiation as a function of μ. Same as Fig. 6 except that the range of the azimuthal angle is $30° < \phi \leq 60°$ or $120° < \phi \leq 150°$.

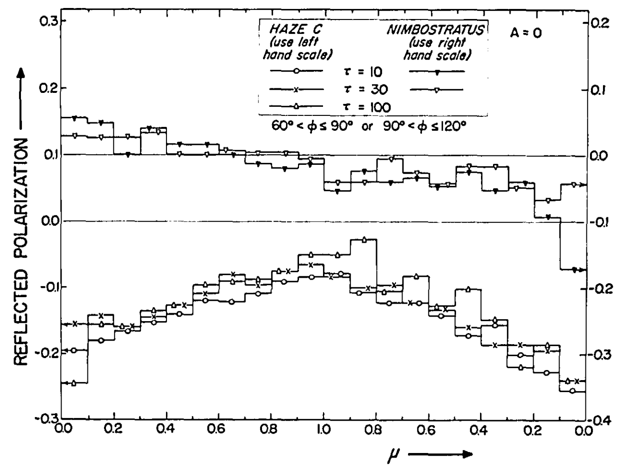

Fig. 8. Polarization of reflected radiation as a function of μ. Same as Fig. 6 except that the range of the azimuthal angle is $60° < \phi \leq 120°$.

curve that changes its shape as τ increases is the one for the case $60° < \phi \leq 120°$; this curve is relatively flat for small values of τ but becomes concave downward for large τ values.

The polarization for the nimbostratus model is particularly interesting; it shows that details of the single scattering matrix are still important for reflection from clouds of large optical thickness. The maximum of the polarization for the interval $0.8 < \mu < 0.7$ on the antisolar side is a feature of all the curves for various τ values ($\tau = 0.1$ and 1 in Figs. 18 and 19 of Ref. 20, and $\tau = 10$ and 30 in Fig. 6 here). This is not a fluctuation in the Monte Carlo results, but rather occurs at the appropriate angle that includes the single scattered photons scattered through a 140° scattering angle. This corresponds to the maximum in the single scattered polarization curve shown in Fig. 15 of Ref. 20. This maximum value is reduced from approximately 0.49 when $\tau = 0.1$ to 0.13 when $\tau = 30$. For all values of τ, the polarization for the nimbostratus model is slightly positive near the solar horizon, then is negative until near the nadir where it becomes strongly positive, and then finally becomes negative once again for angles nearer the antisolar horizon. The polarization curve when $30° < \phi \leq 60°$ or $120° < \phi \leq 150°$ is slightly positive near the solar horizon and then crosses over near the nadir and assumes fairly large negative values as the antisolar horizon is approached.

With the Rubenson definition of the degree of polarization, the perpendicular and parallel components of the radiance are measured with respect to the plane which contains both the incident and scattered directions. Thus the photons scattered from a direction near the nadir and with $\phi = 90°$ have a polarization equal in absolute value, but of opposite sign, to those also scattered near the nadir, but with $\phi = 0°$. A comparison of our curves shows that this condition is approximately satisfied. The deviations are caused mainly by the intervals in both μ and ϕ over which the results are averaged at the detectors.

The results for the reflected radiance for an intermediate solar angle such that $\mu_0 = -0.55$ are given in Fig. 9 for the nimbostratus model. The reflected radiance shows much less variation with both nadir and azimuthal angle at this solar angle than for the two cases already discussed. The reflected polarization is shown in Fig. 10. Once again there is relatively little variation with both nadir and azimuthal angle. Many of the variations in this curve are caused by the single scattering matrix for the nimbostratus model and are not fluctuations in the Monte Carlo calculations. For example, the peak in the curve for $0° < \phi \leq 30°$ or $150° < \phi \leq 180°$ for the interval $1.0 < \mu < 0.9$ on the antisolar side of the nadir is caused by the maximum in the single scattered polarization which occurs for a scattering angle near 140°. Single scattered photons which are scattered through this angle are detected in this μ interval.

Mean Optical Path

The optical path of photon is defined as the sum of the optical thicknesses for each segment of the photon trajectory. The mean optical path of the reflected photons is the mean value of the optical path for all photons that leave the atmosphere through the upper boundary. The mean optical paths of both the reflected and transmitted photons are given in Table I.

The reflected mean optical path increases as the cloud thickness increases and decreases as the incident solar beam moves from the zenith to the horizon. When the reflected mean optical paths for the haze C and nimbostratus models are compared, the values are

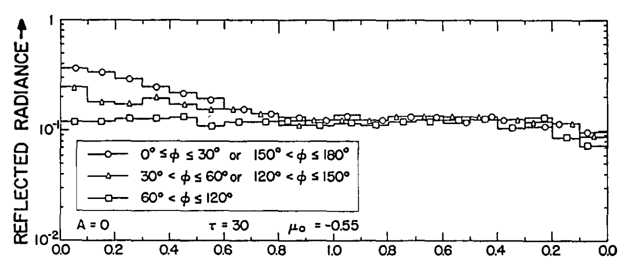

Fig. 9. Reflected radiance as a function of μ for nimbostratus model, $\mu_0 = -0.55$, $\tau = 30$, $A = 0$, and various ranges of azimuthal angle.

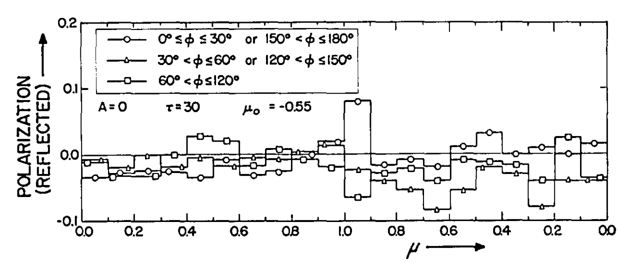

Fig. 10. Polarization of reflected radiation as a function of μ for nimbostratus model, $\mu_0 = -0.55$, $\tau = 30$, $A = 0$, and various ranges of azimuthal angle.

Table I. Mean Optical Path, Flux at Lower Boundary for A = 0, and Cloud Albedo for A = 0

Model	τ	μ_0	Reflected mean optical path	Transmitted mean optical path	Diffuse flux at lower boundary, $A = 0$	Cloud albedo, $A = 0$
Haze *C*	10	−1	24.3	23.9	−0.435	0.564
Haze *C*	30	−1	43.3	77.9	−0.186	0.827
Haze *C*	100	−1	87.6	795	−0.034	0.921
Haze *C*	10	−0.15	12.2	27.6	−0.180	0.820
Haze *C*	30	−0.15	23.1	99.0	−0.081	0.920
Haze *C*	100	−0.15	39.7	871	−0.024	0.987
Nimbostratus	10	−1	26.6	18.1	−0.636	0.364
Nimbostratus	30	−1	56.1	65.4	−0.327	0.678
Nimbostratus	100	−1	110	654	−0.113	0.875
Nimbostratus	30	−0.55	42.8	79.8	−0.225	0.771
Nimbostratus	10	−0.15	14.8	27.6	−0.264	0.733
Nimbostratus	30	−0.15	27.6	83.1	−0.136	0.867

always greater for the nimbostratus model. This is because the photons penetrate, on the average, deeper into the cloud with the nimbostratus model because of the greater probability of small angle forward scattering.

The transmitted mean optical path increases with the optical thickness of the cloud. For the haze *C* model and $\mu_0 = -1$, the transmitted mean optical path is 23.9 when $\tau = 10$ and 795 when $\tau = 100$. It increases slightly as the solar beam moves from the zenith to the horizon. The corresponding values are less for the nimbostratus model than for the haze *C* model, because of the reason already mentioned.

Diffuse Flux and Cloud Albedo

The diffuse flux at the lower boundary when $A = 0$ is given in Table I. This is the total flux received minus the contribution from unscattered photons of the beam. The diffuse flux, besides exhibiting the expected decrease with increasing τ and decreasing μ_0, is less in each case for the haze *C* model than for the nimbostratus model. This effect results from the much greater forward small angle scattering in the nimbostratus model compared to the haze *C* model.

The cloud albedo is defined as the fraction of the incident flux which is reflected from the cloud through its upper boundary for a surface albedo of zero. The cloud albedo increases with increasing τ and decreasing μ_0. In each case the cloud albedo is less for the nimbostratus model than for the haze *C* model. This results from the greater probability for scattering through angles greater than 90° for the haze *C* model than for the nimbostratus model.

Comparison with Experimental Measurements

Quantitative comparisons between published values for the reflected radiance and our calculations are not possible because the measurements are made for different solar zenith angles, over a wavelength range from 0.55 μ to 0.85 μ (in a typical case), from clouds with an unknown optical thickness and with an unknown drop size distribution, and for an unknown surface albedo below the clouds. However, in spite of these uncertainties certain general features of the experimental results are evident.

When the sun is near the horizon, measurements (see Figs. 6 and 7 of Ref. 12, Fig. A.5 of Ref. 11, and Fig. 7 of Ref. 10) of the reflected radiance in the principal plane give values which are six to ten times greater near the solar horizon than at the nadir and which increase only moderately toward the antisolar horizon. This agrees with the trend of the curves shown in Fig. 3. These same measurements indicate that the radiance increases only by a factor of 1.5 to 2 from the nadir to the horizon when the azimuthal angle is near 90°. Again, this agrees with the calculated curves shown in Fig. 5.

Experimental measurements in the range of solar zenith angles from 50° to 68° (see Fig. 8 of Ref. 12, Fig. A.3 of Ref. 11, and Fig. 6 of Ref. 10) may be compared approximately with our calculations for a solar zenith angle of 56.6° (Fig. 9). These measurements for this range of solar zenith angles indicate that the reflected radiance increases by a factor of 2.5 to 4 from the nadir to the solar horizon in the principal plane and increases by only a small amount from the nadir to the antisolar horizon. There is little variation in the measured radiance when the azimuthal angle is 90°. These measurements agree with our calculated results shown in Fig. 9.

Very few measurements have been published which can be compared with Fig. 1 for the sun at the zenith. Measurements of Salomonson (Ref. 11, Fig. A.1) made for a solar zenith angle of 16–17° show the reflected radiance decreasing toward the horizon. The decrease becomes more pronounced according to our calculations as the sun approaches closer to the zenith.

References

1. H. C. van de Hulst and K. Grossman, "Multiple Light Scattering in Planetary Atmospheres" in *The Atmospheres of Venus and Mars*, J. C. Brandt and M. B. McElroy, Eds. (Gordon and Breach, New York, 1968), pp. 35–55.
2. J. E. Hansen, Astrophy. J. **155**, 565 (1969).
3. J. E. Hansen, J. Atmos. Sci. **26**, 478 (1969).
4. J. E. Hansen, Astrophy. J. **158**, 337 (1969).
5. R. E. Danielson, D. R. Moore, and H. C. van de Hulst, J. Atmos. Sci. **26**, 1078 (1969).
6. A. Uesugi and W. M. Irvine, Astrophy. J. **159**, 127 (1970).
7. W. M. Irvine, Astrophys. J. **152**, 823 (1968).
8. S. Twomey, H. Jacobowitz, and H. B. Howell, J. Atmos. Sci. **24**, 70 (1967).
9. M. Neiburger, J. Meteorol. **6**, 98 (1949).
10. I. Ruff, R. Koffler, S. Fritz, J. S. Winston, and P. K. Rao, J. Atmos. Sci. **25**, 323 (1968).
11. V. V. Salomonson, "Anisotropy in Reflected Solar Radiation," Atmospheric Science Paper No. 128, Colorado State U., Fort Collins, Colo. (1968).
12. B. Brennan and W. R. Bandeen, Appl. Opt. **9**, 405 (1970).
13. G. N. Plass and G. W. Kattawar, Appl. Opt. **7**, 361 (1968).
14. G. N. Plass and G. W. Kattawar, Appl. Opt. **7**, 415 (1968).

15. G. N. Plass and G. W. Kattawar, Appl. Opt. **7**, 699 (1968).
16. G. W. Kattawar and G. N. Plass, Appl. Opt. **7**, 869 (1968).
17. G. N. Plass and G. W. Kattawar, Appl. Opt. **8**, 2489 (1969).
18. D. Deirmendjian, Appl. Opt. **3**, 187 (1964).
19. G. W. Kattawar and G. N. Plass, Appl. Opt. **6**, 1377 (1967).
20. G. W. Kattawar and G. N. Plass, Appl. Opt. **7**, 1519 (1968).

OSA Research and Education

On 14 May 1970 the U. S. National Commission for UNESCO and the National Science Foundation jointly convened a meeting of some forty persons representing scientific and educational societies and other organizations concerned with scientific and technological education. The purpose of the meeting was to tell us about the Division of Science Teaching of UNESCO and to elicit our interest in its work.

The term *UNESCO* is one of the acronyms more or less taken for granted these days. It is short for United Nations Educational, Scientific and Cultural Organization. If we had been asked for a quick answer, we might have guessed that the *S* stands for *social*, which indeed it does, in a way, in the clear recognition by UNESCO of the importance of the scientific and technological competence of developing countries to their general social development.

Robert H. Maybury, a member of the UNESCO Division of Science Teaching since 1960, now on leave to Harvard Project Physics, and Albert V. Baez, a former director of the Division, talked about UNESCO with convincing enthusiasm. They emphasized that the operating principle of this intergovernmental program is based on the people-to-people concept, and they spoke of the rewarding nature of the work of the science teaching program to American college and university faculty members who have helped with it for short tours of one or two years. Some college teachers spend a sabbatical year in the service of UNESCO. Others take a leave of absence from their institutions.

It was emphasized that the work involves far more than the transfer of modern scientific and technological expertise to teachers and students in developing countries. That is a part of the work, and an important part. Equally important is what Maybury called "the delivery system," which involves a perceptiveness to the motivations of a people, how they go about their work, and what it takes to arouse their interest in a subject. The general objective involves both the training of scientific and technological personnel in a country and the development of organizational and planning activities to make for a self-sustaining program without perpetual administration by the United Nations.

In the same vein, Baez spoke of UNESCO as being basically a catalyzer and internationalizer. Often, a small program strikes a spark of interest which later leads to a national program of significance in one of the developing countries.

One way in which UNESCO and the scientific societies can assist each other is through closer acquaintance. Toward that end, UNESCO urges individual scientists to make use of their facility in Paris. For example, scientists planning to visit Europe or Asia may write in advance to the Division of Science Teaching and ask for the names of individuals and scientific institutions engaged in their specialty in the countries they plan to visit. The Division will even help make arrangements in advance for visits to some of these places. UNESCO cordially invites travelers to visit it in Paris to make use of the Briefing Room, which is a sort of clearinghouse for educational materials, such as journals, audiovisual systems, and other pertinent items. The address for personal inquiries or visits is Division of Science Teaching, UNESCO, Place de Fontenoy, 75 Paris 7^e, France..

There are several things that scientific societies, and especially their individual members, can do to help the UNESCO. One of these is to publicize help the Division of Science Teaching can provide to visitors, which we have just done in the preceding paragraph. Another is to interest American teachers in volunteering for service with UNESCO for two years, a year, or even a semester. We conclude that the number of billets is relatively small. While the enthusiasm of Maybury and Baez would lead many highspirited teachers to apply for UNESCO positions, pursuit of the subject revealed that there are now only thirty Americans in the UNESCO Science Teaching Program, although the U. S. Office of Education may receive some 2000 inquiries each year from individuals interested in or curious about the program. Of those who inquire, perhaps a few hundred names will ultimately be forwarded to UNESCO, where they will be added to similar lists from other nations. Thus, representatives of the Office of Education and the Department of State properly warned that this appealing international program is not blessed with an unlimited number of positions to offer to science teachers.

We have given the UNESCO address in Paris for personal inquiries and visits. It is appropriate also to give the address of the American group responsible for U. S. activities in UNESCO: U. S. National Commission for UNESCO, Department of State, Washington, D.C. 20520. We hope that some OSA members will wish to write to one or both for direct information, if they feel inclined toward service with UNESCO.

The Optical Society of America is, of course, thoroughly international. The last issue of the *Directory* J. Opt. Soc. Amer. 59, Auguest, Part 2 (1969) listed 573 foreign members in forty countries—about 10% of total membership at that time. Nearly half of the Honorary Members of the Society have been elected from the foreign membership, as well as many of the medalists. Cooperation with UNESCO would serve to promote the principles and purposes of the Society, and we shall publish other information about the Science Teaching Program as it becomes available.

John A. Sanderson
Research & Education Officer